Thermochimica Acta, 53 (1982) 125–139
Elsevier Scientific Publishing Company, Amsterdam—Printed in The Netherlands

STRUCTURAL AND SURFACE ASPECTS OF THERMALLY TREATED PHOSPHATED AND SULPHATED SILICA GEL

ANWAR AMIN

Department of Chemistry, Faculty of Education, Ain Shams University, Cairo (Egypt)

SAID HANAFI and SUZY A. SELIM *

Department of Chemistry, Faculty of Science, Ain Shams University, Cairo (Egypt)

(Received 23 July 1981)

ABSTRACT

Silica gel submitted to phosphate and sulphate treatments and heated in the temperature range 150–600°C has been studied by adsorption of N_2 at −195°C and C_6H_{12} and CH_3OH at 35°C. Structural characterizations were performed by XRD and TG.

Silica gel, impregnated with ammonium phosphate solution and heated to 300°C forms $(NH_4)_8H_2(P_3O_{10})_2 \cdot 3\,H_2O$, with characteristic bands at *d*-distances of 5.305 Å, 3.08 Å and 3.76 Å. At 150°C, bands at 4.33 Å and 3.91 Å may point to a condensed phosphate adsorbed on silica.

Dimerization of $(NH_4)_2SO_4$ is favoured upon adsorption on silica and $(NH_4)_3H(SO_4)_2$ is the main product at 300°C. At 600°C, both impregnated silica species are amorphous to X-rays.

Thermal treatment of phosphated silica is accompanied by a continuous decrease in N_2-areas whereas the reverse results from sulphate treatment. Phosphation appears to favour dehydroxylation and enhances sintering.

The organic probe molecules do not measure the true area. Methanol adsorption is largely affected by the decomposition products of the impregnating salts on the surface at temperatures <500°C as well as the pore size at ≥ 500°C. Sites especially active towards methanol adsorption are thought to be present in phosphated silica at 500°C, above which temperature they are lyophobic towards cyclohexane.

Pore structure analysis from N_2-adsorption data shows that phosphate treatment blocks some of the narrower pores leading to higher average pore radii compared with the sulphated samples. Shrinkage of phosphated silica commences at 500°C.

1. INTRODUCTION

The modification of silica surfaces to meet the various industrial requirements was mainly focused on their treatment with a halogen (chlorination or fluorination), in an attempt to produce a catalyst with greater catalytic activity and selectivity [1] through changes in the surface acidity [2,3].

The use of phosphate as an impregnating anion for silica modification also

* To whom correspondence should be addressed.

0040-6031/82/0000–0000/$02.75

increased its acidity [1] but the effect of the sulphate anion on pure silica was not investigated though it has remarkably altered both the acidity and acid strength of other oxide systems [4].

In addition to changes in the acidity of the silica surface, phosphate treatment bears especial significance as a fertilizer and in sandy grounds its effect on the water uptake and pore sizes should not be ignored. As physical adsorption must precede chemical interaction, it follows that the hydroxyl group is likely to be the most important one in the formation of corresponding stable surface compounds, as it is for other oxide systems [5,6].

The role of these impregnating anions on the texture of silica is thus an essential parameter for the complete understanding of their function. In a previous publication [7], the effect of fluorination was investigated and in the present investigation the impregnation of ammonium sulphate and ammonium phosphate onto silica gel is studied using N_2 and CH_3OH adsorption. Structural characterisation of the samples were achieved by the use of XRD and TG.

2. EXPERIMENTAL

The silica gel (59) employed in this investigation was supplied by the Davidson Division of W.R. Grace and Co. precharacterized to contain only wide pores [8].

A sample (PS) impregnated with phosphate ions was prepared by soaking 10 g of the silica gel in 100 ml of a 0.6509 M solution of diammonium hydrogen phosphate (B.D.H.) prepared by dissolving the salt in ammonia solution of pH > 11. The solid was then decanted and dried at 110°C overnight.

Another sample (SS) was impregnated with sulphate ions adopting the same conditions as sample (PS) and using a 0.6509 M ammonium sulphate (B.D.H.) solution only.

Dehydration products were obtained by heating in the presence of air for 5 h over the temperature range 150–600°C. Henceforth, the temperature will always follow the sample label in specifying a certain product.

X-Ray diffraction patterns are obtained by means of a Philips X-ray diffractometer model PW 1010 using Ni filtered Cu Kα radiation.

Thermogravimetric analysis was carried out in static air using Stanton Redcroft thermobalance type 750/770, the heating rate being 5° min^{-1}.

Adsorption–desorption isotherms of nitrogen at -195°C and of cyclohexane and methanol at 35°C were determined by conventional gas adsorption.

3. RESULTS

3.1 X-Ray and Thermogravimetry

The XRD pattern of sample PS-110 is poorly crystalline (Fig. 1) and traces of $(NH_4)_2HPO_4$ could be detected. A broad band in the region of low 2θ values from

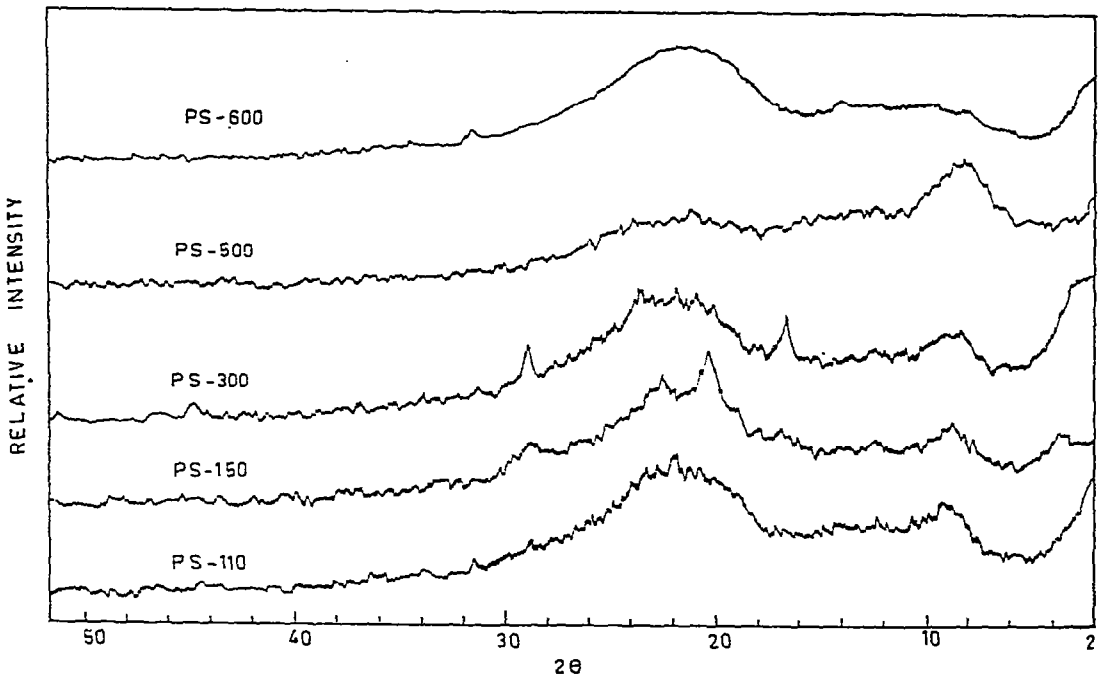

Fig. 1. X-Ray diffraction patterns for phosphated silica gel (PS) and its thermally treated products.

7° to 11° is also observed. Upon heating to 150°C two main bands appeared at *d*-distances of 4.33 Å and 3.91 Å besides several small bands in the region of low 2θ values being comparable with those of PS-110. These two bands together do not point to any known compound of ammonium phosphate [9] or to any corresponding compound with silica [9]. At 300°C, these bands disappeared and a product with two different main bands at 5.3 Å and 3.08 Å resulted together with bands of lower intensities at 3.74 Å and 10.78 Å (Fig. 1) which are also unidentified. At 500°C, the crystallinity decreased markedly and the very weak bands present may point to some interaction between the phosphorous oxide formed at this temperature and silica, may be SiP_2O_7 ($SiO_2 \cdot P_2O_5$), which decomposes at 600°C leaving behind amorphous silica.

To elucidate the structure of these products, TG analysis of sample PS and pure $(NH_4)_2HPO_4$ were carried out (Fig. 2). Three steps are observed for sample PS, the first step is terminated at ~180°C with a weight loss of ~4.6% followed by a clear small inflection at 275°C and the last step continued up to 1000°C with a total loss of 9.8%. TG of $(NH_4)_2HPO_4$ showed three distinct steps (Fig. 2, curve (b)). The first step is completed at 160°C and remained unaffected by thermal treatment up to 200°C with 10.85% loss in weight followed by a gradual decomposition up to ~560°C above which the rate of decomposition increased and is almost completed at ~680°C.

The XRD pattern of a sample of $(NH_4)_2HPO_4$ heated at 170°C for 3 h in the presence of air is different from any known compound of ammonium phosphate and

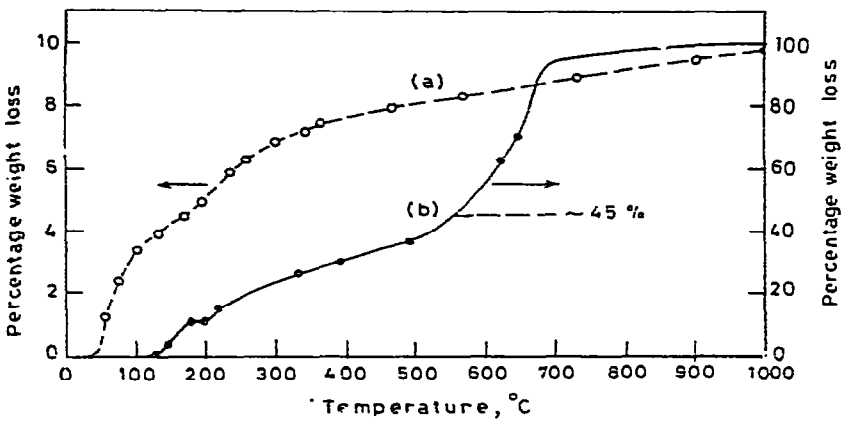

Fig. 2. Thermogravimetric curves for phosphated silica (curve a) and $(NH_4)_2HPO_4$ (curve b).

possessed bands, the most characteristic and intense of which are at 3.08 Å, 5.305 Å and 3.77 Å, respectively (Fig. 3). The decomposition of $(NH_4)_2HPO_4$ to an extent of ~ 10.85% would only be produced according to the equation

$$6\,(NH_4)_2HPO_4 \rightarrow \underset{\text{Product A}}{(NH_4)_8H_2(P_3O_{10})_2 \cdot 3\,H_2O} + 4\,NH_3 + H_2O \text{ (theoretical loss 10.86\%)}$$

and so the pattern obtained is believed to correspond to this product, $(NH_4)_8H_2(P_3O_{10})_2 \cdot 3\,H_2O$. Above 200°C, it decomposed gradually evolving ammonia and water leaving behind P_2O_5 at ~ 560°C above which it evaporated (m.p. 563°C) [10]. At this temperature the material has undergone a loss of ~ 45.5% which

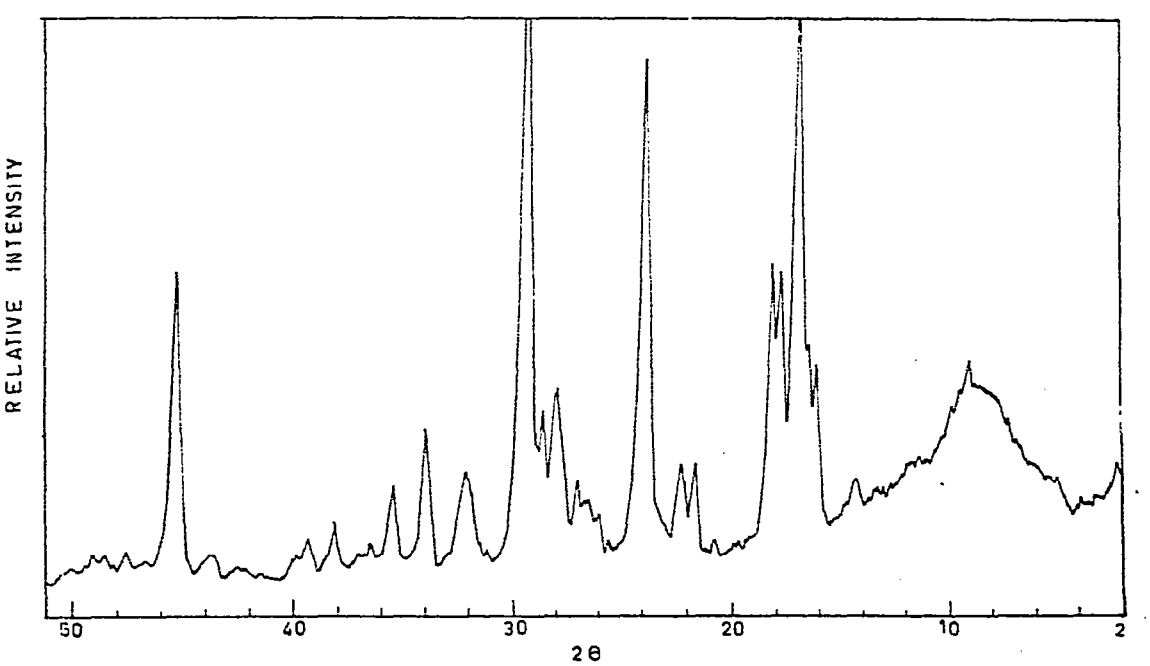

Fig. 3. X-Ray diffraction pattern of $(NH_4)_2HPO_4$ heated at 170°C for 3 h.

is in close agreement with the theoretical value of 46.23% for the formation of 3 P_2O_5 from 6 $(NH_4)_2HPO_4$.

The characteristic X-ray bands for the product PS-300 coincided with those of product (A). However sample PS-150 did not show any bands characteristic of $(NH_4)_2HPO_4$ though traces of it were observed in sample PS-110. Recalling that the original silica was soaked in $(NH_4)_2HPO_4$ in the presence of a high ammonia concentration (pH >11), a phosphate with high ammonia content, probably the triammonium phosphate, may have formed in a condensed (polymerised) state in the silica surface together with some excess ammonia adsorbed on the surface. Heating at 110°C would thus cause the evolution of both adsorbed ammonia and H-bonded water, whereas heating at 150°C developed the crystalline pattern of the condensed phosphate, probably a condensed triammonium phosphate adsorbed on the surface. This adsorbed phosphate is decomposed in the temperature range 180–270°C (the second small step) to give the pattern of $(NH_4)_8H_2(P_3O_{10})_2 \cdot 3\,H_2O$ at 300°C. Above this temperature it decomposed continuously and heating at 500°C for 5 h seemed sufficient to cause its complete decomposition leaving P_2O_5 on the surface.

The XRD pattern of the original sample SS showed the presence of ammonium sulphate on the silica surface together with a broad band in the 2θ range of about 7–10° (Fig. 4). At 150°C, the presence of $(NH_4)_2SO_4$ is no longer recognized and the main band at a d-distance of 4.038 Å does not belong to any related compound. Meanwhile, the intensity of the band in the low 2θ range is increased. At 300°C the

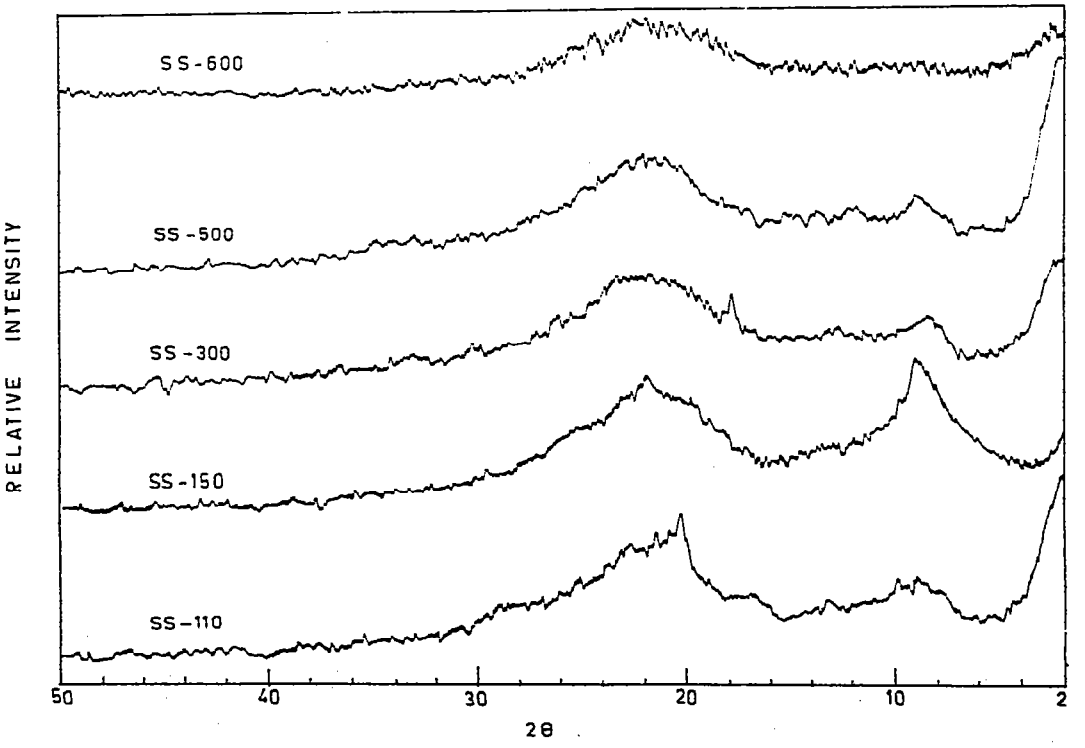

Fig. 4. X-Ray diffraction patterns of sulphated silica gel (SS) and its thermally treated products.

product is identified as $(NH_4)_3H(SO_4)_2$ and the band at low 2θ values is markedly reduced. Above this temperature the crystallinity decreased and the product at 600°C is amorphous.

The TG of sample SS showed three distinct steps—one commencing at ~50°C and terminating at ~230°C with about 5.7% weight loss followed by a small but distinct step which terminated at about 350°C partially overlapping with the last step which terminated at about 950°C giving a total loss of 18.97% (Fig. 5, curve (a)). TG of pure ammonium sulphate (Fig. 5, curve (b)) carried out under the same atmospheric condition (static air) showed that it commenced decomposition at 438°C with an inflection at ~575°C corresponding to about 13% decomposition (theoretical loss for the formation of NH_4HSO_4 is 12.87%).

Complete decomposition is accomplished at ~800°C. Thus the first step in the TG of sample SS is a result of the evolution of the physically adsorbed water present in the silica. The second small step resulted from the evolution of one ammonia molecule from two molecules of $(NH_4)_2SO_4$ to form $(NH_4)_3H(SO_4)_2$ as identified for sample SS-300. The XRD pattern of sample SS-150 seems to correspond to that of the dimerized ammonium sulphate adsorbed on the surface. The adsorbed $(NH_4)_3H(SO_4)_2$ then decomposed continuously at higher temperatures. Thus thermal treatment of adsorbed $(NH_4)_2SO_4$ on the silica surface formed the intermediate product $(NH_4)_3HSO_4$ and not NH_4HSO_4.

Comparing the TGA data of samples PS and SS, the total weight loss is found to

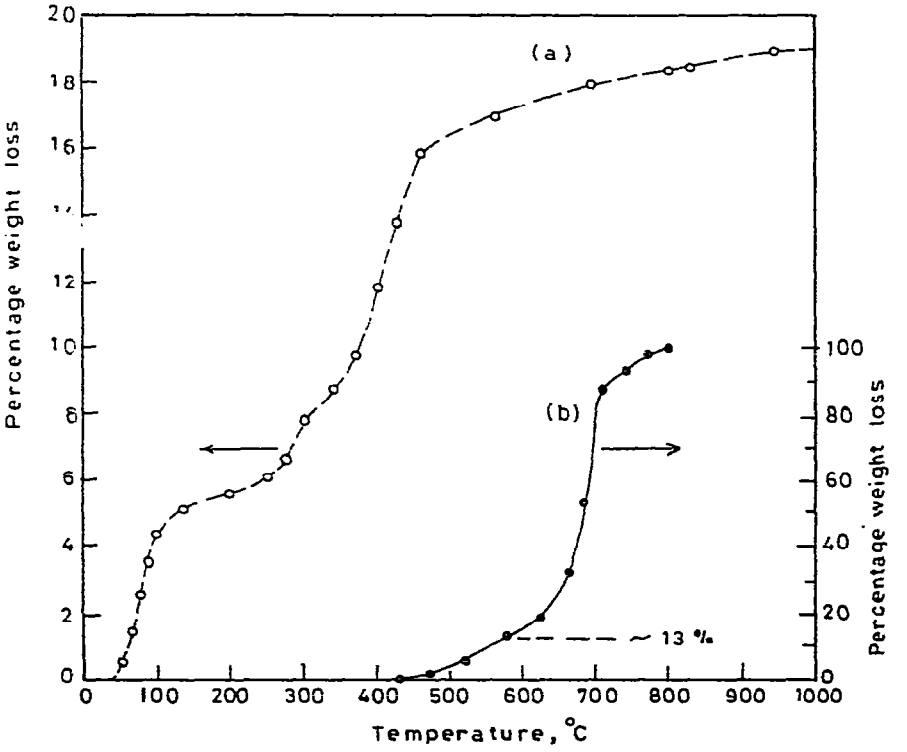

Fig. 5. Thermogravimetric curves for sulphated silica gel (curve a) and $(NH_4)_2SO_4$ (curve b).

be 9.8% and 18.97%, respectively, in spite of the use of identical conditions regarding silica weights, molarity of impregnating solutions, soaking period and temperature. This points to the greater adsorption of the sulphate over the phosphate which may partly arise from differences in the pH of the soaking medium [11].

3.2 N_2 adsorption

Adsorption–desorption isotherms of nitrogen obtained for the phosphated (PS) and sulphated (SS) silicas thermally treated at different temperatures are all type II. The phosphated silica sample exhibited a reversible hysteresis loop which is persistent with heat treatment up to 500°C and became very narrow at 600°C. This trend is different from that previously reported [7] for the pure silica soaked in distilled water.

The isotherms obtained for the sulphated silica (SS) and its heated products are completely reversible and no capillary condensation is observed. The disappearance of the hysteresis loop upon the introduction of anions was also observed for low F^- concentrations on the same silica [7] and also by other oxide systems [12]. The presence or absence of the capillary condensation reflects clearly the active contribution of the phosphate and sulphate anions towards affecting the pore dimension of the products.

The specific surface areas are estimated by the application of the BET equation over its normal range of applicability and by adopting a value of 16.2 $Å^2$ as the molecular area of adsorbed nitrogen.

The specific surface areas and BET-C constants of the above samples are given in Table 1, columns 2 and 4.

Both phosphation and sulphation decreased the area markedly for samples

TABLE 1

Surface characteristics of phosphated (PS) and sulphated (SS) silica gels obtained from N_2 adsorption

Sample	$S_{BET}^{N_2}$ ($m^2\,gm^{-1}$)	$S_t^{N_2}$ ($m^2\,gm^{-1}$)	BET-*C* constant	$V_{P(0.93)}$ ($ml\,gm^{-1}$)	$r_{H(0.93)}$ (Å)
PS-150	336.9	340.0	24	0.4711	13.983
PS-300	292.6	291.0	17	0.4508	15.406
PS-500	261.0	258.0	14	0.3900	14.940
PS-600	244.1	255.0	13	0.3198	13.100
SS-150	309.2	310.0	24	0.3588	11.600
SS-300	342.2	345.0	20	0.4165	12.170
SS-500	380.7	395.0	25	0.4571	12.010
SS-600	413.6	418.0	24	0.4485	10.840

heated at 150°C as compared with the pure gel, the latter being more effective (Fig. 6). At this temperature, an increase in area would have been expected since from TG the loss in weight up to 150°C is greater for these samples than for the corresponding pure silica soaked in water and adjusted to a comparable pH [13]. However since these samples are originally dried at 110°C, this increase in weight loss arises from its exposure to the atmosphere which signifies the greater hydrophilic character of the sulphated silica over the phosphated silica. From total pore volume data taken at $P/P^0 = 0.95$ ($V_{p_{0.95}}$) and average pore radii obtained as $\bar{r}_H = V_{p_{0.95}}/S_{BET}$ (Table 1, columns 5 and 6, respectively) a decrease is observed in both these parameters for samples PS-150 and SS-150 compared with that of the untreated silica [7]. The impregnating ions thus appear to enter into the pore system and block completely some of the narrower pores. From TG the adsorption of silica to the impregnating sulphate ions exceeds that for the phosphate (section 3.1), thereby giving rise to lower values for S_{BET}, $V_{p_{0.95}}$ and $\bar{r}_H$ which is concordant with the results obtained.

Thermal treatment of phosphated silica up to 600°C is accompanied by a continuous decrease in area whereas the reverse took place with sulphated silica. The fluctuations of specific area with treatment temperature previously observed for the pure silica soaked in water and arising from the evolution of H-bonded and bulk hydroxyls are no longer observed (Fig. 6). Heat treatment of sample PS continuously gave rise to volatile or gaseous products (Fig. 2, curve a) which was expected to

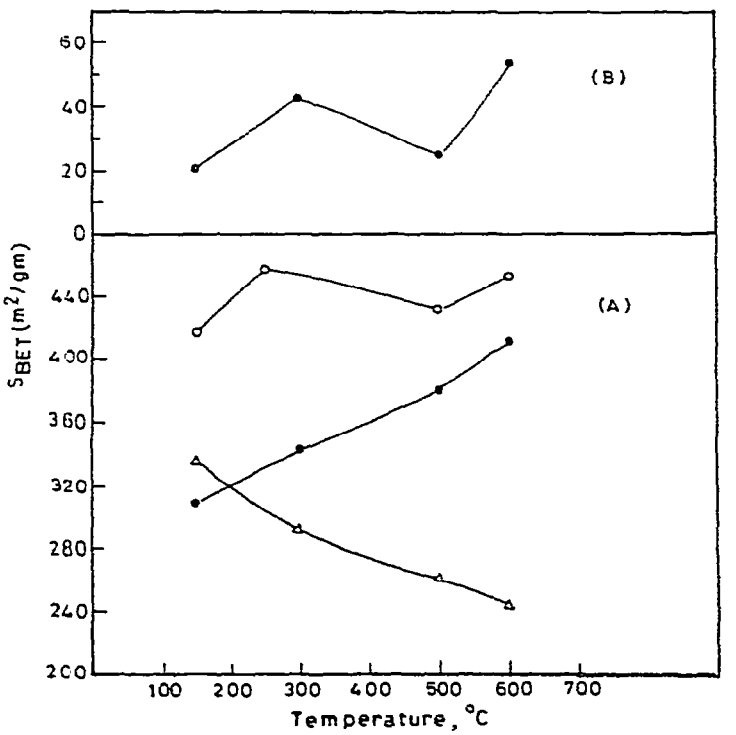

Fig. 6. Variation of specific surface area with treatment temperature. (A) From N_2 adsorption data: △, phosphated silica; ●, sulphated silica; ○, silica soaked in water (for sake of comparison [7]. (B) From C_6H_{12} adsorption on sulphated silica.

produce an increase in area and not a decrease. The total pore volume data (Table 1, column 5) showed a continuous decrease whereas the average pore radius (column 6) indicated some widening at 300°C followed by a continuous narrowing of the pore system. It appears that at 300°C, the effects brought about by the chemical and physical properties of the compound $(NH_4)_8H_2(P_3O_{10})_2 \cdot 3\,H_2O$, also reflected by the change in BET-C constant (Table 1, column 4), outweighs that produced by the evolution of either its decomposition products or even the evolved water from the H-bonded hydroxyls [7]. At this temperature some of the narrower pores are completely blocked by the formation of this "macromolecule" giving rise to an increased value for $\bar{r}_H$.

Above 300°C, the presence of the dehydrating oxide P_2O_5 on the surface seemed to contribute to the dehydroxylation of any H-bonded or bulk hydroxyls. The continuous decrease observed in the surface parameters $S_{BET}^{N_2}$, $V_{p_{0.95}}$ and $\bar{r}_{H_{0.95}}$ indicated shrinkage of the solid matrix whereby an enhanced sintering effect is taking place.

The situation is different with sample SS, where the increase in area up to 500°C is accompanied by an increase in $V_{p_{0.95}}$ and to a smaller extent in $\bar{r}_H$, being nearly the same at 300 and 500°C, pointing to the continuous creation of pores by the decomposition products evolved (Table 1, columns 5 and 6). The nature of the surface appears to be stable along the temperature range investigated, the BET-C constant remaining in the range 20–25 (Table 1, column 4).

At 600°C, the evolution of the remaining decomposition products (Fig. 5) and of any adsorbed species of the previously evolved gases, causes the creation of some narrower pores at the expense of the wider ones giving rise to a decrease in both $V_{p_{0.95}}$ and $\bar{r}_H$ together with a larger increase in $S_{BET}^{N_2}$ than previously obtained at lower temperatures.

These modifications in the surface texture were also reproduced from the pore structure analysis using the *t*-method of de Boer et al. [14] to detect and differentiate between the existence of micro- and mesopores in the samples. In these plots, the *t*-curves of Mikhail et al. [15] based on non-porous solids with low BET-C constants which matched those of the samples under test were used. The agreement between S_t and S_{BET} is observed for all samples (Table 1, columns 3 and 2, respectively) showing the *t*-curve used in the analysis to be correct. A typical set of V_l–*t* plots constructed for the heated products of the phosphated and sulphated samples from N_2 adsorption is shown in Fig. 7 (a) and (b), respectively.

From these plots, an upward deviation is found to commence at a *t*-value of 6 Å for samples from PS and SS heated to 150 and 300°C. This positive deviation does not continue and reverts back at a *t*-value of 11.8 Å and 10 Å, respectively, where the samples form a mixed pore system. Though two regions of upward deviations were previously observed at 4 Å and 6 Å for the pure gel soaked in water [7], only one region is found upon phosphation or sulphation where the impregnating ions completely blocked the groups of narrower pores as previously mentioned. Besides, the slope of the upward deviation does not increase to the same extent as it does for the pure gel, which points to a narrowing of the pores present, the effect being

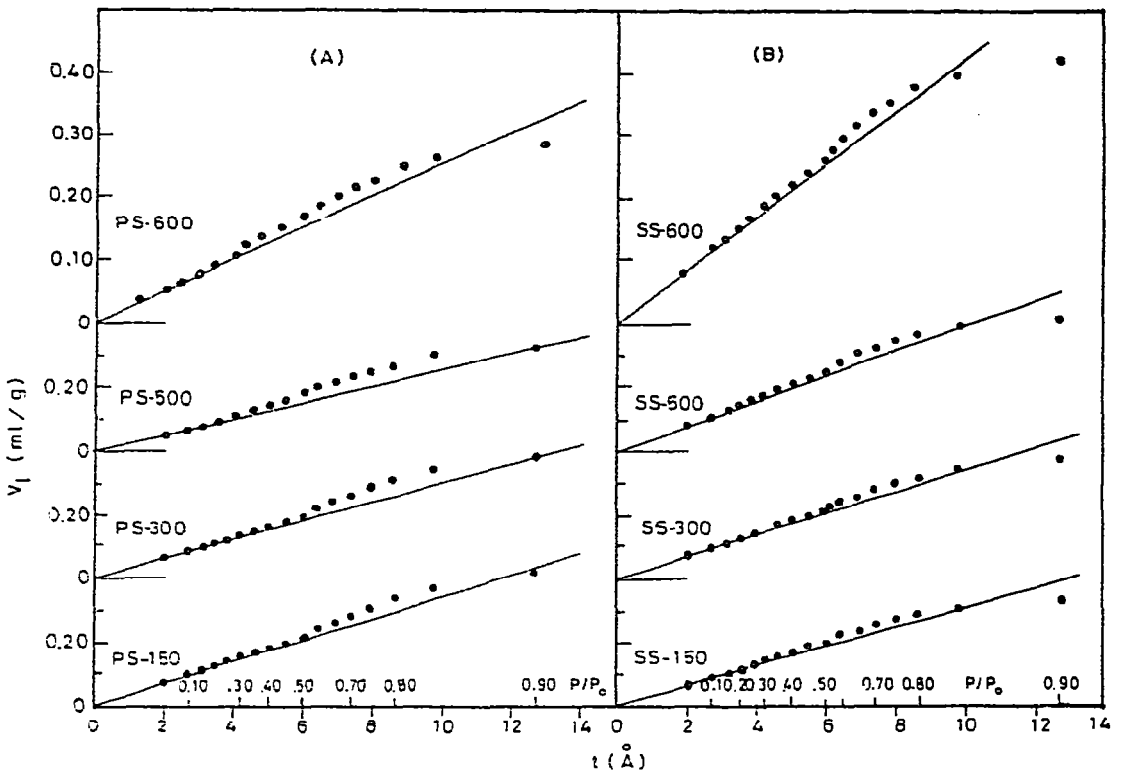

Fig. 7. V_l–t plots for the thermally treated products of phosphated (a) and sulphated (b) silica gel from nitrogen adsorption.

greater with sulphation. This increased narrowing of products from (SS) is reflected in the adsorption isotherms where the absence of hysteresis loops indicates pore dimensions which would not permit capillary condensation to take place. These plots thus reflect the same picture previously arrived at from r_H data (Table 1, column 6). However, at temperatures $\geqslant 500°C$, this second group of mesopores make their appearance for products from PS upon the decomposition of the adsorbed species of the impregnating material. Products from SS do not show up this group clearly.

3.3 Cyclohexane and methanol adsorption

Full adsorption–desorption cycles of cyclohexane and methanol are obtained for the thermally treated products of samples PS and SS.

The cyclohexane isotherm of the product from sample PS treated at 150°C is type III which changes to type II at 300°C then to type V at higher temperatures. Those obtained for products from SS are all type IV. The isotherms are characterized by very low adsorption in the BET region and very high adsorption at $P/P_0 > 0.70$ where adsorbate–adsorbate interaction is significant. All the isotherms obtained exhibit closed hysteresis loops whose shapes are characteristic of type A of de Boer's classification [16] showing two very steep branches similar to that observed upon fluorination of this silica [7].

The methanol isotherms obtained for all products from PS and SS are type II. The isotherms obtained for samples PS-150 and PS-300 are characterized by high adsorption at $P/P_0 < 0.05$ followed by a small constant region of adsorption which is then followed by multilayer adsorption. These observations reflect the highly specific nature of the adsorption of methanol on these two samples, as will be further confirmed from analysis of their pore structure.

All methanol isotherms exhibit hysteresis loops except sample SS-150 where hysteresis is absent. The relative pressures at which closure of the hysteresis loops occurred varied. The lowest relative pressure at which closure took place, was at $P/P_0 \sim 0.30$ for products from PS heated at temperatures $\geqslant 300°C$.

Surface areas are evaluated from the isotherms of type II or type IV by the use of the BET equation and adopting a value of 39 Å^2 and 25 Å^2 for the molecular areas of cyclohexane and methanol, respectively. For methanol, this value was proposed for the adsorption on amorphous silica surfaces [17].

Area values obtained from type III or V isotherms are unreliable and therefore no correlation could be achieved from the cyclohexane data of products from PS.

Products from SS give extremely low cyclohexane area values because most of the pores are inaccessible to the cyclohexane molecules. Cyclohexane possesses nearly the same tendency for attraction to the silica surface as nitrogen [18] and the very low adsorption at low relative pressures arises from steric effects where most of the pores are too small to take up the cyclohexane molecules. Nevertheless, from the variations of specific area with treatment temperature (Fig. 6(B)) the increase observed at 300°C results from the widening of the pores, as noted from the $\bar{r}_H$ values from N_2 adsorption data (Table 1, column 6) thereby increasing the accessibility towards cyclohexane adsorption. The increase in area at 600°C results from the evolution of pores with dimensions that permit the cyclohexane molecules to penetrate (section 3.2), thereby producing higher area values compared with those of SS-500, in spite of their comparable nature—both showing an identical BET-C constant, namely 8.

The methanol areas produced for the various samples, $S_{BET}^{CH_3OH}$, are much lower than the corresponding N_2-areas, $S_{BET}^{N_2}$, which are assumed to measure correctly the total surface area of the samples, indicating a certain specificity in the adsorption of methanol molecules on the surface.

For samples heated to $\leqslant 300°C$, the methanol areas for samples from SS are higher than those from PS, though, according to the $\bar{r}_H$ values produced from N_2-adsorption data (Table 1, column 6) the reverse should have taken place. From total pore volume data, $V_{p_{0.95}}$ obtained from methanol adsorption (Table 2, column 6) samples from PS show lower values than from SS which is the reverse of what was observed from N_2-adsorption data. This situation could however arise if the condensed phosphate molecules are situated on opposite and adjacent sites in these pores as well as at their entrances. Upon the adsorption of the methanol molecules, which, being polar, are strongly attracted to these condensed phosphate molecules which themselves seem to be easily polarized, narrowing at the pore entrances as well as in their interior occurs. This specific adsorption, taking place predominantly at

TABLE 2

Surface characteristics of phosphated (PS) and sulphated (SS) silica gel obtained from methanol adsorption

Sample	BET-C constant	$S_{BET}^{CH_3OH}$ ($m^2\,gm^{-1}$)	$S_t^{CH_3OH}$ ($m^2\,gm^{-1}$)	Number of moles adsorbed at monolayer	$V_{p(0.95)}$ ($ml\,gm^{-1}$)
PS-150	76	154.0	153	1.027×10^{-3}	0.1933
PS-300	151	155.4	156	1.036×10^{-3}	0.1996
PS-500	47	199.5	199	1.329×10^{-3}	0.3032
PS-600	9	151.0	–	1.384×10^{-3}	0.3411
SS-150	121	193.9	192.0	1.295×10^{-3}	0.1945
SS-300	81	193.0	196.0	1.288×10^{-3}	0.2931
SS-500	141	166.0	174.0	1.109×10^{-3}	0.2425
SS-600	35	189.0	192.0	1.265×10^{-3}	0.3537

pressures below 0.05 P/P_0 as observed from the high initial adsorption in the corresponding isotherms, not only hinders the deep penetration of methanol into the pores but also blocks some of them as will be observed later in their V_1–t plots.

On the other hand, the dimerized sulphate seems to be more homogeneously distributed and less polarizable, thus facilitating the entrance of the methanol to the inside of these pores and measuring more area than is available for the phosphated silica. The effect of these impregnating ions on the solid surface of samples heated at 300°C with regard to methanol adsorption seemed to compensate for the expected decrease in area arising from the decrease in polarizability of the silica surface resulting from the evolution of the adsorbed water [19] thus keeping the area nearly constant.

At 500°C, the area changed remarkably for both samples, decreasing for SS-500 and increasing for PS-500. In the temperature range 300–500°C, decomposition of the surface compounds $(NH_4)_3H(SO_4)_2$ and $(NH_4)_8H_2(P_3O_{10})\cdot 3\,H_2O$ (section 3.1) took place, probably leaving behind some adsorbed sulphur and phosphorus oxides, respectively, together with some sites, produced upon their desorption, which are active towards methanol adsorption, as found for products heated at 600°C.

In the temperature range 500–600°C, the chemical nature of the solid surface is no longer the main controlling parameter, and the pore dimension then becomes significant resulting in higher areas for methanol adsorption on samples of PS where widening of the pores is evident from the V_1–t plot of PS-500, discussed later.

The effect of phosphation or sulphation towards CH_3OH adsorption is better visualized if the number of moles adsorbed at the monolayer (Table 2, column 5) is compared with the data previously obtained for the pure gel [7]. Samples heated at $\leqslant 300$°C show lower or nearly the same (as SS-300) values as those produced from the corresponding pure silica gel, but at temperatures $\geqslant 500$°C sulphation or phosphation increases the number of moles adsorbed, the effect being more significant for the latter treatment. Thus at e.g. 600°C, the number of moles of methanol

adsorbed on the pure, sulphated and phosphated gel are 1.075, 1.265 and 1.384, respectively. These results signify that either new sites become available for methanol adsorption or the sites already present become more easily polarisable and possess increased affinity towards methanol adsorption thereby favouring the formation of polarisable hydrogen bonds between the adsorbate molecules themselves [30].

The changes brought about in the nature of the surface are also reflected on the pore structure of the solid as demonstrated by their V_l–t plots. In these plots, the t-curve of Mikhail et al. [21] based on samples with the BET-C constant covering the range 14–75 is adopted. The pore analysis is determined for all samples except sample PS-600 whose BET-C constant, being 9, is lower than that of the reference material upon which the t-curve is based.

The agreement between $S_{BET}^{CH_3OH}$ and $S_t^{CH_3OH}$ (Table 2, columns 3 and 4, respectively) was observed for the above samples fulfilling the required criterion for the correct choice of the t-curve.

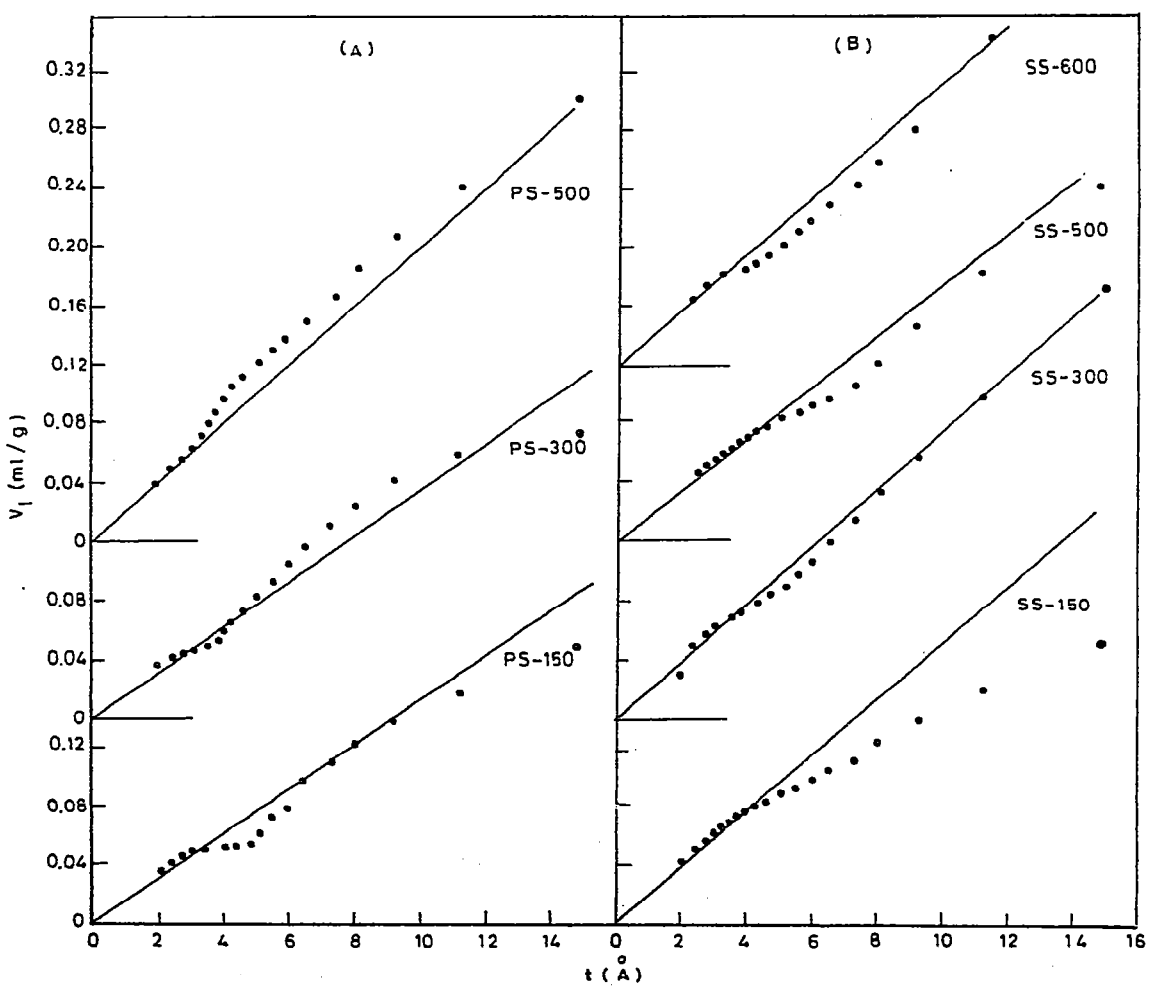

Fig. 8. V_l–t plots for the thermally treated products of phosphated (a) and sulphated (b) silica gel from methanol adsorption.

The main characteristics of these V_1-t plots may be summarized in the following.

(1) Samples PS-150 and PS-300 show a downward deviation at a t-value of ~ 3 Å resulting in a marked decrease in slope which does not continue and the slope increases at t-values of 4.7 Å and 4 Å, respectively (Fig. 8) reverting back at higher t-values pointing to the co-existence of both meso- and micropores with respect to methanol. The initial downward deviation observed in these two samples reproduced the previous speculation of pore filling where the high specificity of methanol adsorption inside and at the pores' entrances caused their blocking. At higher coverages the adsorption takes place in the outer system and in the wider pores. This sharp downward deviation is not present in samples SS-150 and SS-300 but a gradual decrease in slope is observed at a t-value of ~ 4 Å for both samples, and at t-values of 7 Å and 5.5 Å the slope increases again. This data points to some widening upon heating at 300°C.

2) Sample PS-500 shows widening of the pores by the initial increase in slope observed at $t \approx 3$ Å which remains constant at $t \geqslant 4.5$ Å. Samples SS-500 and SS-600 on the other hand show a negative deviation at $t \approx 5$ Å and 3.5 Å, respectively. However, the subsequent increase in slope at t-values of 7 Å and 5 Å for these two samples indicate that the solid retains its mixed pore system.

3) It has been shown from N_2-adsorption that the series of samples from SS yield V_1-t plots which deviate positively, and not negatively as was produced from the methanol adsorption data. This indicates that these particular samples possess a peculiar size of pores which behave as wide pores with respect to N_2 and as narrow pores with respect to methanol.

REFERENCES

1 G.P. Damon, J.M. Bonnier and B. Delmon, J. Colloid Interface Sci., 55 (1976) 381.
2 K. Tarama, S. Yoshida, H. Honda and K. Taniguchi, Nippon Kagaku Zasshi, 88 (1967) 148.
3 I.D. Chapman and M.L. Hair, J. Catal., 2 (1963) 145.
4 K. Tanabe, M. Itoh, K. Morishige and H. Hattori, in B. Delmon, P.A. Jacob and G. Poncelet (Eds.), Preparation of Catalysts, Elsevier, Amsterdam, 1976.
5 S.S.S. Rajan, K.W. Perott and W.M.H. Saunders, J. Soil Sci., 25(4) (1974) 438.
6 R.L. Parfitt and R.St.C. Smart, Soil Sci. Soc. Am. Proc. 42(1) (1978) 48.
7 S. Hanafi, S.A. Selim, A. Amin and P.G. Rouxhet, Surface Technol., 13 (1981) 265.
8 R.Sh. Mikhail, S. Brunauer and E.E. Bodor, J. Colloid Interface Sci., 26 (1968) 54.
9 Powder Diffraction File; ASTM Alphabetical Index of Inorganic Compounds, International Center for Diffraction Data, Pennsylvania 19081, U.S.A., 1978.
10 Handbook of Chemistry and Physics, CRC Press, Cleveland, Ohio, 43rd edn., 1961.
11 C.-P. Huang and W. Stumm, Am. Chem. Soc., 12 (2) (1972) 200.
12 S.A. Selim and S. Hanafi, Surface Technology, 12 (1981) 287.
13 S.A. Selim, H.A. Hassan, M. Abd-El-Khalik and R.Sh. Mikhail, Thermochim. Acta, 45 (1981) 349.
14 B.C. Lippens, B.G. Linsen and J.H. de Boer, J. Catal., 3 (1964) 32.
J.H. de Boer, B.G. Linsen and Th.J. Osinga, J. Catal., 4 (1965) 643.
15 R.Sh. Mikhail, N.M. Guindy and S. Hanafi, Egypt J. Chem., Special Issue "Tourky", (1973) 53.
16 J.H. de Boer, in P.H. Everette and F.S. Stone (Eds.), The Structure and Properties of Porous Materials, Colston papers, Vol. 10, Butterworths London, 1958.

17 L.N. Soboleva and A.V. Kiselev, Zh. Fiz. Khim., 32 (1958) 49.
18 R.S. McDonald, Presented at the Pittsburgh Conference on Analytical Chemistry and Applied Spectroscopy, March 2, 1956.
19 C. Okkerse, in B.G. Linsen (Ed.), Physical and Chemical Aspects of Adsorbents and Catalysts, Academic Press, London and New York, 1970.
20 M.I. Cruz, W.E.E. Stone and J.J. Fripiet, J. Phys. Chem., 76 (1978) 3078.
21 R.Sh. Mikhail, S.A. Selim and F. Shebl, Egypt. J. Chem., 19(3) (1976) 405–415.